Optimizing Algal Bloom Through Bioenzyme and Harvesting Control for Bioenergy Purposes in Eutrophic Water Bodies

Fadilah Akbar and Mardlijah

JOURNAL INFO • JAMBURA JOURNAL OF BIOMATHEMATICS
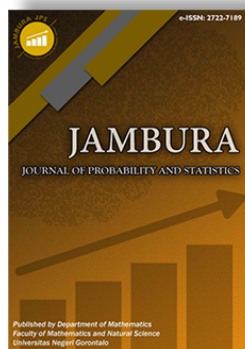
JAMBURA JOURNAL • FIND OUR OTHER JOURNALS

Jambura Journal of Mathematics

Jambura Journal of Mathematics Education

Jambura Journal of Probability and Statistics

EULER : Jurnal Ilmiah Matematika, Sains, dan Teknologi

Research Article

Optimizing Algal Bloom Through Bioenzyme and Harvesting Control for Bioenergy Purposes in Eutrophic Water Bodies

Fadilah Akbar[1] (ID) and Mardlijah[2,*] (ID)

[1,2]Department of Mathematics, Institut Teknologi Sepuluh Nopember, Surabaya 60111, Indonesia
[1]Department of Mathematics, UIN Sunan Ampel Surabaya, Surabaya 60294, Indonesia

ABSTRACT. This article discusses the optimization of algae growth for bioenergy purposes in eutrophic water bodies through bioenzyme control and harvesting. The study explores innovative approaches to manage algae growth in such water bodies. A mathematical model based on dynamical systems, specifically the NASC (Nutrients, Algae, Detritus, and Dissolved Oxygen) algae growth model, was used for the analysis. The results indicate that the system used is unstable, given the needs of algae growth over time. To optimize algae growth, this study proposes controlling the bioenzyme (u_1) feeding to decompose detritus into nutrients and harvesting algae using (u_2). The Pontryagin Maximum Principle (PMP) method was used to obtain optimization with control parameters $u_1 = 0.093$ and $u_2 = 0.32$. The results show that the optimal time to harvest algae is every 84 days or 2.8 months, with an estimated harvestable amount of 16.3667 mg/l. This discovery enhances our understanding of controlling algae growth in the context of renewable energy and reinforces the mathematical approach to managing eutrophic aquatic ecosystems.

1. Introduction

Eutrophication, the increase of nutrients in water bodies, is a significant problem in water resources management, particularly in Indonesia, a country with a vast water area. Chemical waste discharged from various industrial plants has caused waters in Indonesia to become dense with nutrients such as nitrogen and phosphorus [1, 2]. Excessive nutrients in water can cause uncontrolled algae growth, leading to ecological and health problems. This growth reduces sunlight and oxygen levels, creating a "dead zone" that cannot support aquatic life.

Controlling algae growth is crucial for maintaining the balance of the aquatic ecosystem. Optimal control not only improves water quality but also provides benefits in renewable energy through the use of algae oil extracts [3, 4]. The goal is to use these extracts as biodiesel to replace fossil fuels, which is a more environmentally friendly and affordable option. Lipid extracts from algae have various applications, including beauty products, food supplements, and other beneficial products [5]. Algae can also be utilized as a renewable energy source, and it is important to optimize their use in bioenergy, particularly in Indonesia where conditions are favorable for algae growth.

In eutrophic aquatic ecosystems, algae growth is influenced by three main components: nutrients dissolved in water, detritus as deposits of dead organic waste or decomposed organic matter, and dissolved oxygen levels. Actions that can optimize algae growth include providing bioenzymes. The goal is for the bioenzymes to decompose detritus that settles, producing nutrients that will help algae growth. Research on optimizing algae growth using bioenzymes is still rare. Once the algae are sufficient and ready, the next step is harvesting.

Several previous studies have discussed optimizing algae growth. For example, [6] researched optimizing microalgae growth by controlling light intensity using the Linear Quadratic Regulator (LQR) method. [7] also researched optimizing algae growth by controlling nutrients and carbon dioxide (CO_2) in water using LQR and the firefly algorithm. This study will utilize the Maximum Pontryagin Principle (PMP) optimal control method. PMP has the advantage of producing analytic results without the use of randomly generated elements such as LQR. The purpose of using PMP is to obtain precise control without the element of randomness introduced by trial and error. This minimizes the error resulting from the trial and error process [8, 9].

2. Methods

This scientific article will present the findings of research conducted with the objective of optimizing the growth of algae in eutrophic water bodies for the purpose of bioenergy production. The initial step is to obtain a mathematical model of algae growth in eutrophic water bodies. This is followed by a model analysis stage, which includes identifying the equilibrium point of the system, linearizing the model equation system, and analyzing stability around the equilibrium point. The subsequent step is to devise control mechanisms for the model system. This entails incorporating elements of bioenzyme administration and algae harvesting into the model system, thereby rendering it suitable for bioenergy applications. Following the design of the control for the system, the model system will be subjected to preliminary testing to ascertain its degree of control.
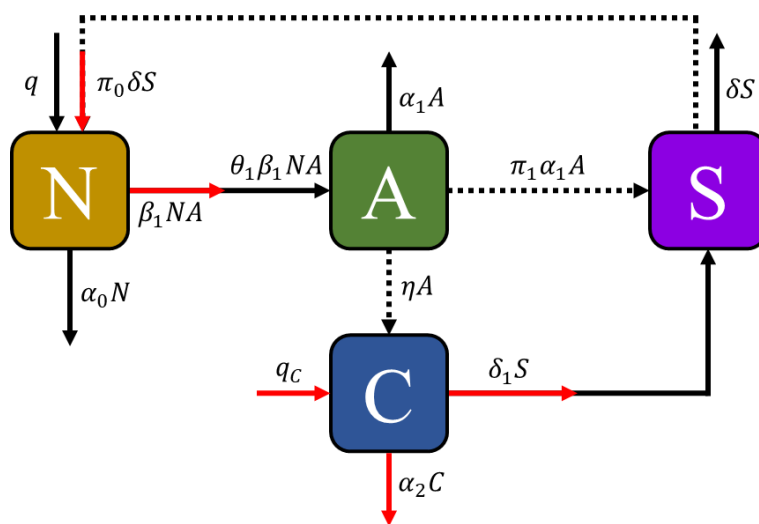
---

*Corresponding Author.

© 2024 by the Author(s).

Figure 1. Compartment Diagram of Model System

Table 1. Summary of the Parameters in Model

Parameters	Parameters Description	Values	Units
q	Nutrient natural depletion rate	0.5	$mgl^{-1}day^{-1}$
α_0	Algae natural depletion rates	0.005	day^{-1}
α_1	Natural depletion rate of algae	0.025	day^{-1}
α_2	Natural depletion rate of dissolved oxygen	0.01	day^{-1}
$\beta 1$	Rate of nutrient depletion due to algae growth	0.4	$mgl^{-1}day^{-1}$
π_0	Nutrient growth rate due to detritus	0.02	-
π_1	Detritus growth rate due to algae	0.9	-
δ	Detritus depletion rate due to decomposing	0.04	day^{-1}
δ_1	Dissolved oxygen depletion rate due to detritus	0.06	day^{-1}
θ_1	Algae growth rate due to nutrients	0.9	-
η	Dissolved oxygen increasing ratedue to algae	0.02	day^{-1}
q_C	Dissolved oxygen increasing rate by various sources	0.2	$mgl^{-1}day^{-1}$

Once the model has been fully controlled, the next step is to perform optimal control on the model system using the Maximum Pontryagin Principle (PMP) method. The primary objective of utilising optimal control with PMP is to obtain the anticipated control variables with precision, without any elements generated randomly through trial and error. This is to minimise the error resulting from the trial and error process.

Once the desired control value has been obtained, the next step is to perform numerical simulations on the model system as a whole. The numerical method used to run the simulation is two-stage Runge-Kutta, which is employed to simulate the state equation. The following is an illustration of the numerical simulation of the state equation using two-stage Runge-Kutta:

$$y_{i+1} = y_i + \frac{1}{6}\left(k_1 + 2k_2 + 2k_3 + k_4\right), \tag{1}$$

with

$$
\begin{aligned}
k_1 &= hf\left(t_i, y_i\right), \\
k_2 &= hf\left(t_i + \frac{h}{2}, y_i + \frac{k_1}{2}\right), \\
k_3 &= hf\left(t_i + \frac{h}{2}, y_i + \frac{k_2}{2}\right), \\
k_4 &= hf\left(t_i + h, y_i + k_3\right).
\end{aligned}
\tag{2}
$$

The fourth-order Runge-Kutta method is employed for the numerical solution of the co-state equation, which is derived from the Pontryagin Maximum Principle (PMP) as follows:

$$y_{i+1} = y_i - \frac{1}{6}\left(k_1 + 2k_2 + 2k_3 + k_4\right), \tag{3}$$

with

$$
\begin{aligned}
k_1 &= hf\left(t_{i+1}, y_{i+1}\right), \\
k_2 &= hf\left(t_{i+1} + \frac{h}{2}, y_{i+1} - \frac{k_1}{2}\right), \\
k_3 &= hf\left(t_{i+1} + \frac{h}{2}, y_{i+1} - \frac{k_2}{2}\right), \\
k_4 &= hf\left(t_{i+1} + h, y_{i+1} - k_3\right).
\end{aligned}
\tag{4}
$$

Once the simulation has been completed, the subsequent step is to analyse the results in order to reach the desired conclusions.

3. Results and Discussion

3.1. Mathematical model system

This article employs a mathematical model system that is consistent with the model used in previous research by [10, 11]. The model system consists of four main variables: Nutrients (N), Algae (A), Detritus (S), and Dissolved Oxygen (C) [12, 13]. The dynamic system diagram is presented in Figure 1.

Representing the compartment diagram in Figure 1 mathematically yields the Ordinary Differential Equation System for the
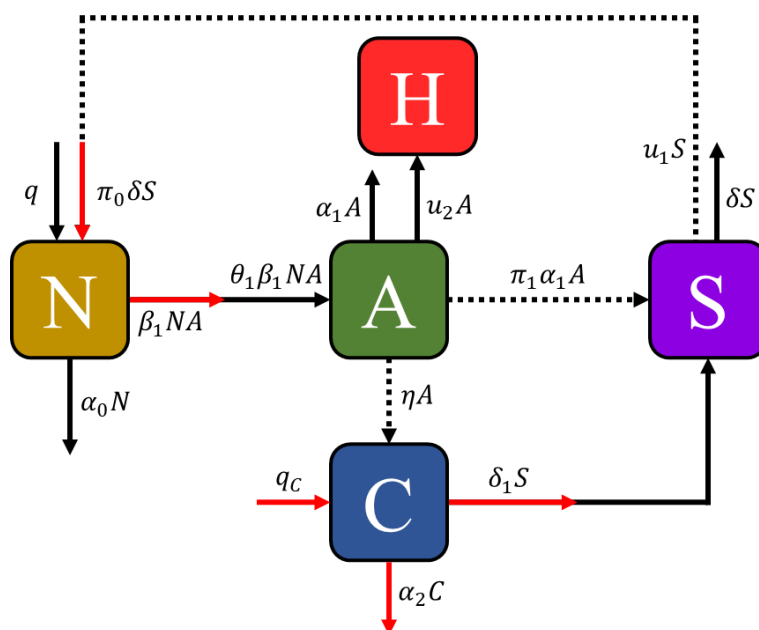
Figure 2. Compartment Diagram of Improved Model System

algae growth model in eutrophic water bodies:

$$\frac{dN(t)}{dt} = q + \pi_0 \delta S - \alpha_0 N - \beta_1 N A_l, \qquad (5)$$

$$\frac{dA_l(t)}{dt} = \theta_1 \beta_1 N A_l - \alpha_1 A_l, \qquad (6)$$

$$\frac{dS(t)}{dt} = \pi_1 \alpha_1 A_l - \delta S, \qquad (7)$$

$$\frac{dC(t)}{dt} = q_C - \alpha_2 C + \eta A_l - \delta_1 S. \qquad (8)$$

The values of the model supporting parameters can be seen in Table 1.

This article proposes the addition of two controls to an existing model system to optimize the growth of algae in eutrophic water bodies for use as bioenergy. The development involves providing bioenzymes to eutrophic waters to accelerate the decomposition of detritus into nutrients and adding a new sub-compartment in the form of $H(t)$, which represents the amount of algae harvested per unit of time [14]. The diagram below illustrates the new compartment of the developed system.

The mathematical form of the compartment diagram in Figure 2 yields the following system of differential equations:

$$\frac{dN(t)}{dt} = q + u_1 S + \pi_0 \delta S - \alpha_0 N - \beta_1 N A_l, \qquad (9)$$

$$\frac{dA_l(t)}{dt} = \theta_1 \beta_1 N A_l - \alpha_1 A_l - u_2 A_l, \qquad (10)$$

$$\frac{dS(t)}{dt} = \pi_1 \alpha_1 A_l - \delta S - u_1 S, \qquad (11)$$

$$\frac{dC(t)}{dt} = q_C - \alpha_2 C + \eta A_l - \delta_1 S, \qquad (12)$$

$$\frac{dH(t)}{dt} = u_2 A_l. \qquad (13)$$

Note that the $H(t)$ sub-compartment serves solely as a monitor for the amount of algae harvested. Therefore, it is only utilized during numerical simulations and is not included in other system analysis models.

1. System Equilibrium Point

At this stage, we seek the equilibrium point of the model system that has been formed. The equilibrium point is obtained by setting eq. (5) to eq. (8) equal to zero $\left(\frac{dN(t)}{dt} = 0, \frac{dA(t)}{dt} = 0, \frac{dS(t)}{dt} = 0, \text{ and } \frac{dC(t)}{dt} = 0 \right)$, resulting in the following [15, 16]:

$$N^* = \frac{\alpha_1}{\beta_1 \theta_1}, \qquad (14)$$

$$A_l^* = \frac{q\beta_1\theta_1 - \alpha_0\alpha_1}{\alpha_1\beta_1 (\pi_0\pi_1\theta_1 - 1)}, \qquad (15)$$

$$S^* = -\frac{(q\beta_1\theta_1 - \alpha_0\alpha_1)\pi_1}{\beta_1 (\pi_0\pi_1\theta_1 - 1)\delta}, \qquad (16)$$

$$C^* = \frac{-\delta\alpha_1\beta_1\pi_0\pi_1 q_C\theta_1 - q\alpha_1\beta_1\delta_1\pi_1\theta_1 + \delta\eta q\beta_1\theta_1}{\alpha_1\beta_1 (\pi_0\pi_1\theta_1 - 1)\delta\alpha_2}$$
$$+ \frac{\alpha_0\alpha_1^2\delta_1\pi_1 - \delta\eta\alpha_0\alpha_1 + \delta\alpha_1\beta_1 q_C}{\alpha_1\beta_1 (\pi_0\pi_1\theta_1 - 1)\delta\alpha_2}. \qquad (17)$$

Substituting the model parameter values into eqs. (14) to (17) yields the equilibrium point values of the model system: $N^* = 0.12$, $A_l^* = 20.93$, $S^* = 58.86$, and $C^* = 291.32$. These equilibrium points will be utilized in the linearization process of the model equation system.

2. Linearization of System Model Equations

The purpose of linearization is to simplify the management and comprehension of the model, particularly around the equilibrium point. Linearizing the system of model equations involves obtaining the analyzed system matrix (A) [15, 17]. This is achieved by deriving a differential equation for each variable in the model system, resulting in the linear form of eqs. (5) to (8) for the equilibrium point in eqs. (14) to (17) as shown in matrix (18).

$$J_A = \begin{bmatrix} \frac{d\dot{N}}{dN} & \frac{d\dot{N}}{dA_l} & \frac{d\dot{N}}{dS} & \frac{d\dot{N}}{dC} \\ \frac{d\dot{A}_l}{dN} & \frac{d\dot{A}_l}{dA_l} & \frac{d\dot{A}_l}{dS} & \frac{d\dot{A}_l}{dC} \\ \frac{d\dot{S}}{dN} & \frac{d\dot{S}}{dA_l} & \frac{d\dot{S}}{dS} & \frac{d\dot{S}}{dC} \\ \frac{d\dot{C}}{dN} & \frac{d\dot{C}}{dA_l} & \frac{d\dot{C}}{dS} & \frac{d\dot{C}}{dC} \end{bmatrix}_{(N^*, A_l^*, S^*, C^*)},$$

$$A = \begin{bmatrix} -\alpha_0 - \beta_1 A_l^* & -\beta_1 N^* & \pi_0 \delta & 0 \\ \theta_1 \beta_1 A_l^* & \theta_1 \beta_1 N^* - \alpha_1 & 0 & 0 \\ 0 & \pi_1 \alpha_1 & -\delta & 0 \\ 0 & \eta & -\delta_1 & -\alpha_2 \end{bmatrix}.$$

$$(18)$$

The subsequent stage involves linearizing the model equation system to derive the control matrix (B) for the system. This matrix will be utilized to determine if the model system can be controlled through the controllability test process. The matrix B is obtained from eqs. (9) to (13) as follows [18]:

$$J_B = \begin{bmatrix} \frac{d\dot{N}}{du_1} & \frac{d\dot{N}}{du_2} \\ \frac{d\dot{A}_l}{du_1} & \frac{d\dot{A}_l}{du_2} \\ \frac{d\dot{S}}{du_1} & \frac{d\dot{S}}{du_2} \\ \frac{d\dot{C}}{du_1} & \frac{d\dot{C}}{du_2} \end{bmatrix}_{(N^*, A^*, S^*, C^*)} \qquad (19)$$

$$B = \begin{bmatrix} S^* & 0 \\ 0 & -A_l^* \\ -S^* & 0 \\ 0 & 0 \end{bmatrix}.$$

3. Stability Analysis of Model System
   Stability analysis is conducted to determine the condition of the system over time. To find the stability condition of a system model, one can calculate the eigenvalues of matrix A. The eigenvalues of matrix A are as follows:

$$|A - \lambda I| = 0.$$

The eigenvalues of the system matrix A are: $\lambda_1 = -0.0100$, $\lambda_2 = 8.3722$, $\lambda_3 = -0.0402$, and $\lambda_4 = -8.3813$. The presence of a positive eigenvalue in the system matrix A indicates that the model system is unstable [19]. This is desirable because an unstable model system results in a constant population, which leads to a shortage of algae for harvesting [20].

3.2. Designing Optimal Control for the System

1. Analysis of System Controllability
   When designing the control for a model system, the first step is to determine whether the system is controllable. To do this, it is necessary to test the controllability of the model system. The following steps should be taken for testing:

$$M_C = \begin{bmatrix} B & Ab & A^2 B & A^3 B \end{bmatrix},$$
$$\text{rank}\,(M_C) = 4.$$

The model system used in this study has a dimension of 4, which means that the value of $n = 4$. Since rank $(M_C) = n$, it can be concluded that the model system is fully controllable (controllability).

2. Pontryagin's Maximum Principle
   To design control with PMP, the initial step is to create an objective function $J(t)$ as the follows [21, 22]:

$$J(u_1(t), u_2(t)) = \int_{t_0}^{t_f} \big(q_1 A(t) + q_2 S(t) + r_1 u_1^2(t) + r_2 u_2^2(t)\big)\, dt,\; q_i \in Q,\; u_i \in U,\; i = 1, 2,$$
$$J(u_1^*, u_2^*) = \max\{J(u_1, u_2)\},$$
$$U = \{u(t), 0 \le u(t) \le 1, \forall t \in [t_0, t_1]\}.$$
$$(20)$$

Once the objective function for optimal control has been established, the subsequent step is to create the Hamiltonian function as in eq. (21) [23, 24].

$$\mathcal{H}(N(t), A(t), S(t), C(t), H(t), u_1(t), u_2(t), \lambda_1(t), \lambda_2, \lambda_3(t), \lambda_4(t), \lambda_5(t), (t))$$
$$=$$
$$(q_1 A(t) + q_2 S(t) + r_1 u_1^2(t) + r_2 u_2^2(t)) + \lambda_1 (q + u_1 S + \pi_0 \delta S - \alpha_0 N - \beta_1 N A_l) + \lambda_2 (\theta_1 \beta_1 N A_l - \alpha_1 A_l - u_2 A_l) + \lambda_3 (\pi_1 \alpha_1 A_l - \delta S - u_1 S) + \lambda_4 (q_C - \alpha_2 C + \eta A_l - \delta_1 S) + \lambda_5 (u_2 A_l).$$
$$(21)$$

To determine the values of the control parameters u_1 and u_2, perform partial derivatives on the Hamiltonian function as in eqs. (22) and (23).

$$\frac{\partial \mathcal{H}}{\partial u_1} = 0,$$
$$2r_1 u_1 + \lambda_1 S - \lambda_3 S = 0,$$
$$2r_1 u_1 - (\lambda_3 - \lambda_1) S = 0,$$
$$2r_1 u_1 = (\lambda_3 - \lambda_1) S,$$
$$u_1^*(t) = \max\left\{0, \min\left\{1, \frac{(\lambda_3 - \lambda_1) S(t)}{2r_1}\right\}\right\},$$
$$(22)$$

$$\frac{\partial \mathcal{H}}{\partial u_2} = 0,$$
$$2r_2 u_2 + \lambda_2 A - \lambda_5 A = 0,$$
$$2r_2 u_2 - (\lambda_2 - \lambda_5) A = 0,$$
$$2r_2 u_2 = (\lambda_2 - \lambda_5) A,$$
$$u_2^*(t) = \max\left\{0, \min\left\{1, \frac{(\lambda_2 - \lambda_5) A(t)}{2r_2}\right\}\right\}.$$
$$(23)$$

After deriving the equations for obtaining control variables u_1 and u_2, the next step is to formulate two equations that play a crucial role in PMP [25]. These equations are used to form the state equations, which are as in eq. (24).

$$N^*(t) = \frac{\partial \mathcal{H}}{d\lambda_1} = q + u_1 S + \pi_0 \delta S - \alpha_0 N - \beta_1 N A_l,$$
$$A^*(t) = \frac{\partial \mathcal{H}}{d\lambda_2} = \theta_1 \beta_1 N A_l - \alpha_1 A_l - u_2 A_l,$$
$$S^*(t) = \frac{\partial \mathcal{H}}{d\lambda_3} = \pi_1 \alpha_1 A_l - \delta S - u_1 S, \qquad (24)$$
$$C^*(t) = \frac{\partial \mathcal{H}}{d\lambda_4} = q_C - \alpha_2 C + \eta A_l - \delta_1 S,$$
$$H^*(t) = \frac{\partial \mathcal{H}}{d\lambda_5} = u_2 A_l,$$

and then formulate the co-state equation as in eq. (25).

$$\lambda_1^*(t) = -\frac{\partial \mathcal{H}}{dN} = -\left(-\lambda_1\left(\alpha_0 + \beta_1 A + \lambda_2 \theta_1 \beta_1 A\right)\right),$$

$$\lambda_2^*(t) = -\frac{\partial \mathcal{H}}{dA} = -\left(q_1 - \lambda_1 \beta_1 N + \lambda_2 \left(\theta_1 \beta_1 N - \alpha_1 - u_2^*\right)\right.$$
$$\left. + \lambda_3 \pi_1 \alpha_1 + \lambda_4 \eta + \lambda_5 u_2^*\right),$$

$$\lambda_3^*(t) = -\frac{\partial \mathcal{H}}{dS} = -\left(q_2 + \lambda_1\left(u_1^* + \pi_0 \delta\right) - \lambda_3\left(\delta + u_1^*\right)\right.$$
$$\left. - \lambda_4 \delta_1\right),$$

$$\lambda_4^*(t) = -\frac{\partial \mathcal{H}}{dC} = \lambda_4 \alpha_2,$$

$$\lambda_5^*(t) = -\frac{\partial \mathcal{H}}{dH} = 0. \tag{25}$$

Once the state and co-state equations are derived, they can be utilized to determine the optimal control and perform numerical simulations of the model system.

3.3. Numerical Simulation

Since the Hamiltonian equation yields two types of equations, namely the state equation and the co-state equation, two solutions are required to obtain the results. To solve both equations, the 4th order Runge-Kutta numerical method is utilized [26]. The 4th order Runge-Kutta forward scheme is used to obtain the solution of the state equation with the following steps as in eq. (26).

$$y_{i+1} = y_i + \frac{1}{6}\left(k_1 + 2k_2 + 2k_3 + k_4\right), \tag{26}$$

where

$$k_1 = hf\left(t_i, y_i\right),$$
$$k_2 = hf\left(t_i + \frac{h}{2}, y_i + \frac{k_1}{2}\right),$$
$$k_3 = hf\left(t_i + \frac{h}{2}, y_i + \frac{k_2}{2}\right),$$
$$k_4 = hf\left(t_i + h, y_i + k_3\right).$$

The co-state equation solution is obtained using the 4th order Runge-Kutta backward scheme, which involves the following steps as in eq. (27).

$$y_{i+1} = y_i - \frac{1}{6}\left(k_1 + 2k_2 + 2k_3 + k_4\right), \tag{27}$$

where

$$k_1 = hf\left(t_{i+1}, y_{i+1}\right),$$
$$k_2 = hf\left(t_{i+1} - \frac{h}{2}, y_{i+1} - \frac{k_1}{2}\right),$$
$$k_3 = hf\left(t_{i+1} - \frac{h}{2}, y_{i+1} - \frac{k_2}{2}\right),$$
$$k_4 = hf\left(t_{i+1} - h, y_{i+1} - k_3\right).$$

The results show that the control of bioenzyme administration yielded a value of $u_1 = 0.093$, while the control in the form of

algae harvesting yielded a value of $u_2 = 0.32$. The following are the simulation results for dissolved oxygen dynamics in Figure 3. The comparison of the amount of dissolved oxygen in eutrophic water bodies is being made between those with and without control in Table 2.
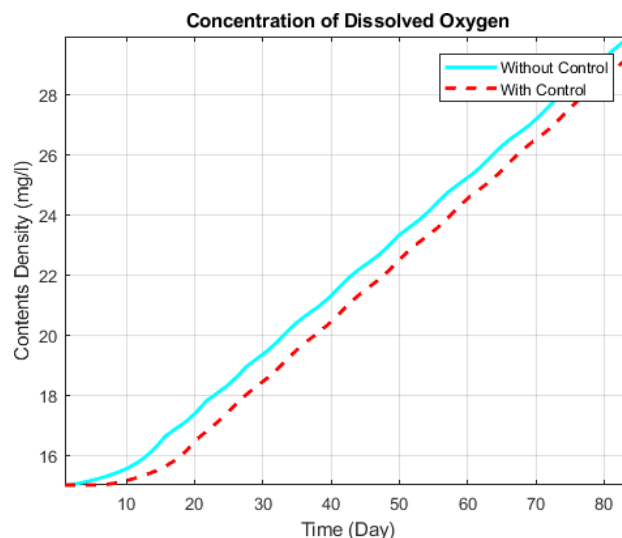

Figure 3. Simulation of Dissolved Oxygen Dynamics

Table 2. Contents Density of Dissolved Oxygen (mg/l)

Days	20	40	60	80
Without Control	17.43	21.36	25.26	29.23
With Control	16.51	20.49	24.57	28.51

The following are the simulation results for detritus dynamics in Figure 4. The amount of detritus in eutrophic water bodies was compared between those with no control and those with control in Table 3.
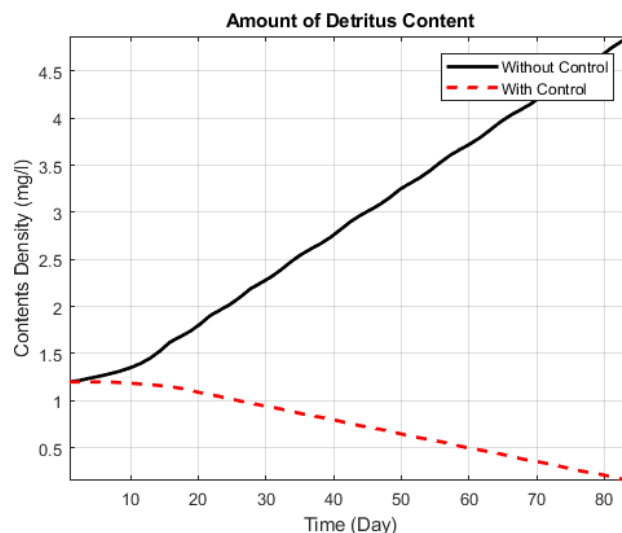

Figure 4. Simulation of Detritus Dynamics

The following are the simulation results for Nutrition dynamics in Figure 5. The comparison of nutrient levels in the eutrophic water body between the control and no control groups is in Table 4.

Table 3. Contents Density of Detritus (mg/l)

Days	20	40	60	80
Without Control	1.812	2.774	3.73	4.701
With Control	1.085	0.793	0.494	0.205
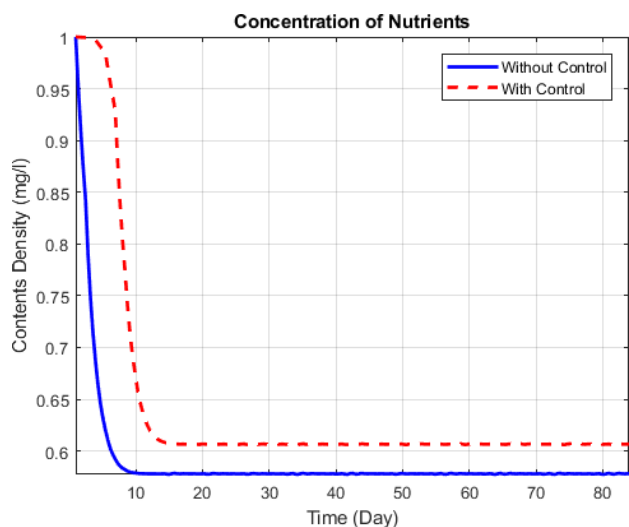
Figure 5. Simulation of Nutrients Dynamics

Table 4. Contents Density of Nutrients (mg/l)

Days	20	40	60	80
Without Control	0.578	0.577	0.578	0.577
With Control	0.607	0.606	0.607	0.606

The simulation results for Algae dynamics are as follows in Figure 6. The comparison of algae levels in eutrophic water bodies between those with and without control measures is in Table 5.
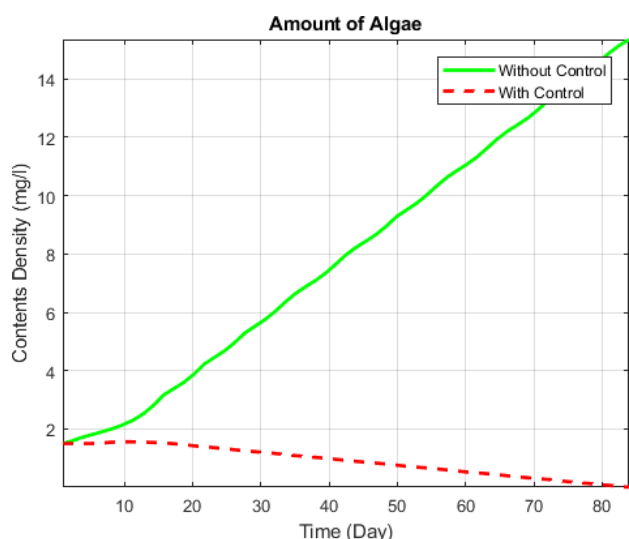

Figure 6. Simulation of Algae Dynamics

Table 5. Contents Density of Algae (mg/l)

Days	20	40	60	80
Without Control	3.889	7.499	11.08	14.72
With Control	1.421	0.978	0.524	0.086

The following are the simulation results for Algae dynamics in Figure 7. The comparison of algae levels in eutrophic water bodies between those with and without control measures is in Table 6.
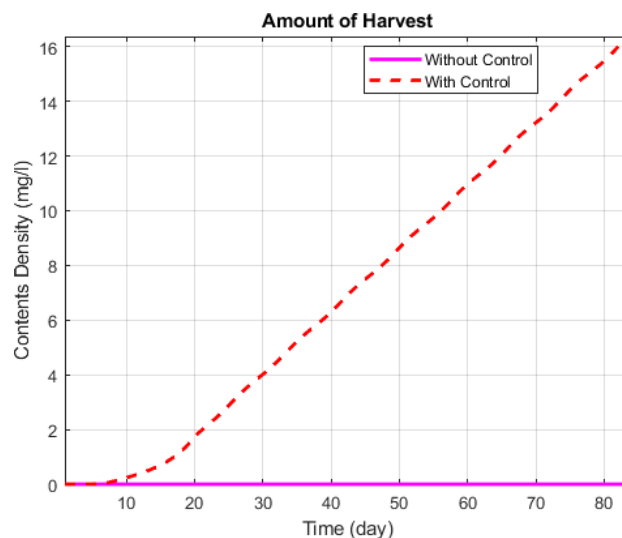

Figure 7. Simulation of Harvest Dynamics

Table 6. Contents Density of Harvest (mg/l)

Days	20	40	60	80
Without Control	0	0	0	0
With Control	1.805	6.355	11.03	15.53

4. Conclusion

Based on the simulation results, controlling the system has a greater impact on the amount of dissolved oxygen in eutrophic water bodies compared to not having control. This is because bioenzymes are provided to aid in the decomposition of detritus into nutrients, causing an increase in the number of algae. This condition is beneficial for aquatic biota, such as fish and other aquatic invertebrates. The provision of bioenzymes is beneficial for the life of aquatic ecosystems in eutrophic water bodies.

Furthermore, based on the simulation results, the amount of detritus when given the control continues to decrease over time due to the effect of decomposition by bioenzymes. So that it makes the amount thinner and turns into nutrients to help algae growth in the eutrophic water body. So that the amount of nutrients contained in the water becomes more and makes the number of algae indirectly also more. The graph shows that the amount of algae when controlled drops dramatically, this is natural because algae are harvested to be used as bioenergy.

Based on the research, the graph in Figure 6 shows that the amount of controlled algae will be depleted within 84 days or 2.8 months. Control is achieved by providing bioenzymes to accelerate the decomposition of detritus into nutrients, which accounts for 9.3% (u_1) of the total detritus content, as well as harvesting 32% (u_2) of the algae. It can be concluded that the optimal time to harvest algae in eutrophic water bodies is once every 84 days or 2.8 months. The estimated amount of harvestable algae is 16.3667 mg/l.

References

[1] A. K. Misra *et al.*, "Dynamics of algae blooming: effects of budget allocation and time delay," *Nonlinear Dynamics*, vol. 100, no. 2, pp. 1779–1807, 2020. DOI:10.1007/s11071-020-05551-4

[2] E. Anagnostou, A. Gianni, and I. Zacharias, "Ecological modeling and eutrophication—A review," *Natural Resource Modeling*, vol. 30, no. 3, pp. 1–27, 2017. DOI:10.1111/nrm.12130

[3] J. K. Mwangi *et al.*, "Microalgae Oil: Algae Cultivation and Harvest, Algae Residue Torrefaction and Diesel Engine Emissions Tests," *Aerosol and Air Quality Research*, vol. 15, no. 1, pp. 81–98, 2015. DOI:10.4209/aaqr.2014.10.0268

[4] M. West *et al.*, "Evaluation of algal bloom mitigation and nutrient removal in floating constructed wetlands with different macrophyte species," *Ecological Engineering*, vol. 108, pp. 581–588, 2017. DOI:10.1016/j.ecoleng.2017.07.033

[5] M. P. Abishek, J. Patel, and A. P. Rajan, "Algae Oil: A Sustainable Renewable Fuel of Future," *Biotechnology Research International*, vol. 2014, pp. 1–8, 2014. DOI:10.1155/2014/272814

[6] Mardlijah, A. Fadhillah, and L. Hanafi, "Performance Analysis of Linear Quadratic Regulator Method in Microalga Growth with Control of Light Intensity," *Journal of Physics: Conference Series*, vol. 1463, no. 1, p. 012004, 2020. DOI:10.1088/1742-6596/1463/1/012004

[7] S. Y. Setyowati and Mardlijah, "Optimal control of microalgae growth using linear quadratic regulator method with firefly algorithm optimization," *Journal of Physics: Conference Series*, vol. 1538, no. 1, p. 012047, 2020. DOI:10.1088/1742-6596/1538/1/012047

[8] Mardlijah *et al.*, "Optimal control of algae growth by controlling CO_2 and nutrition flow using Pontryagin Maximum Principle," *Journal of Physics: Conference Series*, vol. 890, p. 012042, 2017. DOI:10.1088/1742-6596/890/1/012042

[9] Mardlijah *et al.*, "Optimal Control of Lipid Extraction Model on Microalgae Using Linear Quadratic Regulator (LQR) and Pontryagin Maximum Principle (PMP) Methods," *Matematika*, vol. 34, no. 3, pp. 129–140, 2018. DOI:10.11113/matematika.v34.n3.1145

[10] B. M. R. Hasan *et al.*, "Modeling the Effects of Algal Bloom on Dissolved Oxygen in Eutrophic Water Bodies," *Journal of Mathematics*, vol. 2023, pp. 1–20, 2023. DOI:10.1155/2023/2335570

[11] A. B. Janssen *et al.*, "How to model algal blooms in any lake on earth," *Current Opinion in Environmental Sustainability*, vol. 36, pp. 1–10, 2019. DOI:10.1016/j.cosust.2018.09.001

[12] J. B. Shukla, A. K. Misra, and P. Chandra, "Modeling and analysis of the algal bloom in a lake caused by discharge of nutrients," *Applied Mathematics and Computation*, vol. 196, no. 2, pp. 782–790, 2008. DOI:10.1016/j.amc.2007.07.010

[13] C. Tang, Y. Li, and K. Acharya, "Modeling the effects of external nutrient reductions on algal blooms in hyper-eutrophic Lake Taihu, China," *Ecological Engineering*, vol. 94, pp. 164–173, 2016. DOI:10.1016/j.ecoleng.2016.05.068

[14] P. Passy *et al.*, "Eutrophication modelling chain for improved management strategies to prevent algal blooms in the Bay of Seine," *Marine Ecology Progress Series*, vol. 543, pp. 107–125, 2016. DOI:10.3354/meps11533

[15] K. Al-Maqrashi *et al.*, "Mathematical Analysis and Parameter Estimation of a Two-Patch Zika Model," *Letters in Biomathematics*, vol. 10, no. 1, pp. 29–41, 2023.

[16] S. O. S. P. Ahaya, E. Rahmi, and Nurwan, "Analisis dinamik model SVEIR pada penyebaran penyakit campak," *Jambura Journal of Biomathematics (JJBM)*, vol. 1, no. 2, pp. 57–64, 2020. DOI:10.34312/jjbm.v1i2.8482

[17] R. S. Sihaloho and H. Nasution, "Dynamic analysis of SEIR model for Covid-19 spread in Medan," *Jambura Journal of Biomathematics (JJBM)*, vol. 3, no. 2, pp. 68–72, 2022. DOI:10.34312/jjbm.v3i2.16878

[18] P. D. Giamberardino and D. Iacoviello, "A linear quadratic regulator for nonlinear SIRC epidemic model," *2019 23rd International Conference on System Theory, Control and Computing (ICSTCC)* pp. 733–738, 2019. DOI:10.1109/ICSTCC.2019.8885727

[19] E. A. S. Megananda, C. Alfiniyah, and Miswanto, "Analisis kestabilan dan kontrol optimal model matematika penyebaran penyakit Ebola dengan variabel kontrol berupa karantina," *Jambura Journal of Biomathematics (JJBM)*, vol. 2, no. 1, pp. 29–41, 2021. DOI:10.34312/jjbm.v2i1.10258

[20] O. Prosper *et al.*, "Modeling Seasonal Malaria Transmission: A Methodology Connecting Regional Temperatures to Mosquito and Parasite Developmental Traits," *Letters in Biomathematics*, vol. 10, no. 1, pp. 3–27, 2023.

[21] M. L. Olaosebikan, M. K. Kolawole, and K. A. Bashiru, "Transmission Dynamics of Tuberculosis Model with Control Strategies," *Jambura Journal of Biomathematics (JJBM)*, vol. 4, no. 2, pp. 110–118, 2023. DOI:10.37905/jjbm.v4i2.21043

[22] U. Boscain, M. Sigalotti, and D. Sugny, "Introduction to the Pontryagin Maximum Principle for Quantum Optimal Control," *PRX Quantum*, vol. 2, no. 3, p. 030203, 2021. DOI:10.1103/PRXQuantum.2.030203

[23] P. Bettiol and L. Bourdin, "Pontryagin maximum principle for state constrained optimal sampled-data control problems on time scales," *ESAIM – Control, Optimisation and Calculus of Variations*, vol. 27, no. 51, pp. 1–36, 2021. DOI:10.1051/cocv/2021046

[24] N. Kim, S. Cha, and H. Peng, "Optimal control of hybrid electric vehicles based on Pontryagin's minimum principle," *IEEE Transactions on Control Systems Technology*, vol. 19, no. 5, pp. 1279–1287, 2011. DOI:10.1109/TCST.2010.2061232

[25] Y. Liu *et al.*, "Design, Control, and Validation of Two-Speed Clutchless Automatic Transmission for Electric Vehicle," *IEEE/ASME Transactions on Mechatronics*, vol. 27, no. 3, pp. 1299–1310, 2022. DOI:10.1109/TMECH.2021.3086678

[26] L. K. Putri, D. Savitri, and A. Abadi, "Dynamical Behavior in Prey-Predator Model with Mutualistic Protection for Prey," *Jambura Journal of Biomathematics (JJBM)*, vol. 4, no. 2, pp. 103–109, 2023. DOI:10.37905/jjbm.v4i2.21541